analytical chemistry

pubs.acs.org/ac Article

Polyolefin Analyses with a 10 mm Multinuclear NMR Cryoprobe

Zhe Zhou,* Rainer Kuemmerle,* Nathan Rau, Donald Eldred, Aitor Moreno, Barbara Czarniecki, Xiaohua Qiu, Rongjuan Cong, Anthony P. Gies, Leslie Fan, Evelyn Auyeung, Dain B. Beezer, Huong Dau, and Eva Harth

Cite This: *Anal. Chem.* 2020, 92, 15596−15603 Read Online

ACCESS | Metrics & More | Article Recommendations | Supporting Information

ABSTRACT: Polyolefins are important and broadly used materials. Their molecular microstructures have direct impact on macroscopic properties and dictate end-use applications. ^{13}C NMR is a powerful analytical technique used to characterize polyolefin microstructures, such as long-chain branching (LCB), but it suffers from low sensitivity. Although the ^{13}C sensitivity of polyolefin samples can be increased by about 5.5 times with a cryoprobe, when compared with a conventional broadband observe (BBO) probe, further sensitivity enhancement is in high demand for studying increasingly complex polyolefin microstructures. Toward this goal, distortionless enhancement by polarization transfer (DEPT) and refocused insensitive nuclei enhanced by polarization transfer (RINEPT) are explored. The use of hard, regular, and new short adiabatic 180° ^{13}C pulses in DEPT and RINEPT is investigated. It is found that RINEPTs perform better than DEPTs and a sensitivity enhancement of 3.1 can be achieved with RINEPTs. The results of RINEPTs are further analyzed with statistics software JMP and recommendations for optimal usage of RINEPTs are suggested. An example of analyzing saturated chain ends in an ethylene−octene copolymer sample with a hard 180° ^{13}C RINEPT pulse is demonstrated. It is shown that the experimental time can be further reduced in half because of faster proton relaxation, where the total experimental time is about 580 times shorter when compared to using a conventional method and a 10 mm BBO probe. A naturally abundant nitrogen-containing polyolefin is analyzed using $^{1}H-^{15}N$ HMBC and, to our knowledge, is the first $^{1}H-^{15}N$ HMBC presented in the field of polyolefin characterization. The relative amount of similar nitrogen-containing structures is quantified by two-dimensional integration of $^{1}H-^{15}N$ HMBC. Two pragmatic technical challenges related to using high-sensitivity NMR cryoprobes are also addressed: (1) A new ^{1}H decoupling sequence Bi_Waltz_65_256pl is proposed to address decoupling artifacts in $^{13}C\{^{1}H\}$ NMR spectra which contain a strong ^{13}C signal with a high signal-to-noise ratio (S/N). (2) A simple pulse sequence that affords zero-slope spectral baselines and quantitative results is presented to address acoustic ringing that is often associated with high-sensitivity cryoprobe use.

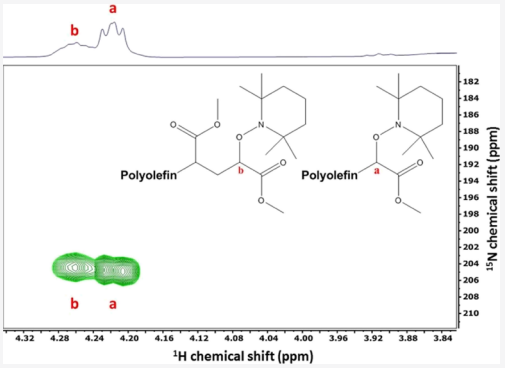

INTRODUCTION

Polyolefins are an important class of materials used in a wide range of products including consumer bags, toys, lamination and agricultural films, packaging, electrical insulation, pipes, footwear, roofing, automotive, fabric, diapers, and bottles for lotion/powder, among many other uses. Polyolefin production exceeds 120 million metric tons every year,[1] with new and improved catalysts/polyolefins constantly being developed.[2−5] Polyolefin microstructures have direct impact on macroscopic properties and dictate end-use applications. ^{13}C NMR is a powerful analytical technique used to characterize polyolefin microstructures, such as long-chain branching (LCB), triad sequence distribution, and blockiness, but it suffers from low sensitivity. One of the ways to increase sensitivity is through the use of cryogenically cooled NMR probes. Cryoprobe technology was proposed by Hoult,[6] and the first commercial products were developed in the 1990s.[7] These products focused on 3−5 mm cryoprobes with an upper temperature limitation of 80 °C and were mainly used in biological research.[8,9] In 2007, a high-temperature 10 mm C/H cryoprobe, capable of reaching 135 °C, was developed by Bruker.[10] This type of cryoprobe has been extensively used for ^{13}C and ^{1}H NMR characterization of polyolefins,[11−18] with over 100 US patents granted using data generated with these cryoprobes.[19−21] In order to meet the diversifying needs of polyolefin and hybrid polyolefin studies, a multinuclear (C−Si−N−P/H) 10 mm high-temperature cryoprobe was recently developed.

Although the NMR sensitivity for polyolefin analysis can be increased dramatically with a cryoprobe, further sensitivity

Received: September 3, 2020
Accepted: October 30, 2020
Published: November 10, 2020

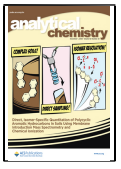

https://dx.doi.org/10.1021/acs.analchem.0c03753
Anal. Chem. 2020, 92, 15596−15603

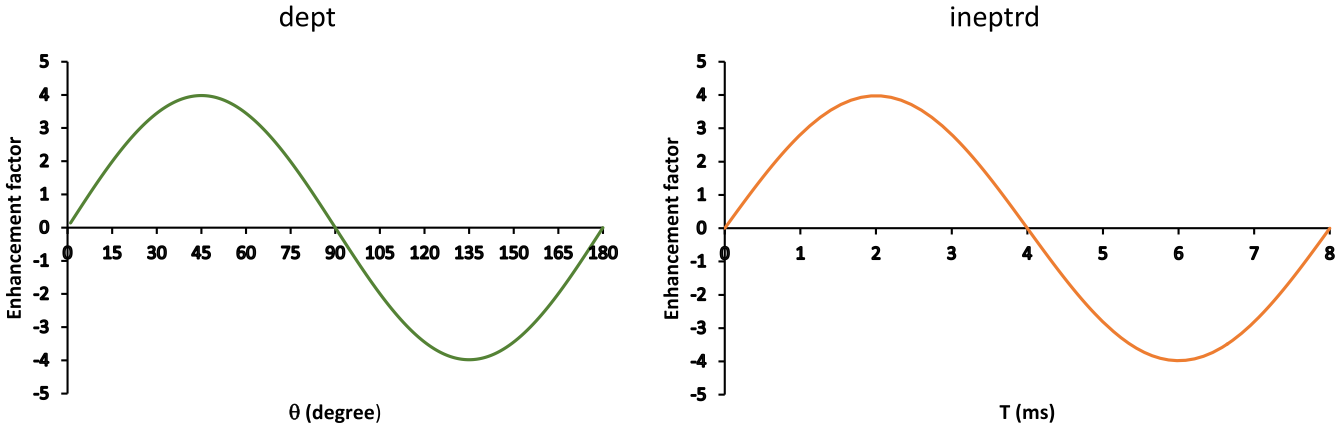

Figure 1. Theoretical signal enhancement factors of DEPTHP (dept) and RINEPTHP (ineptrd) for CH_2.

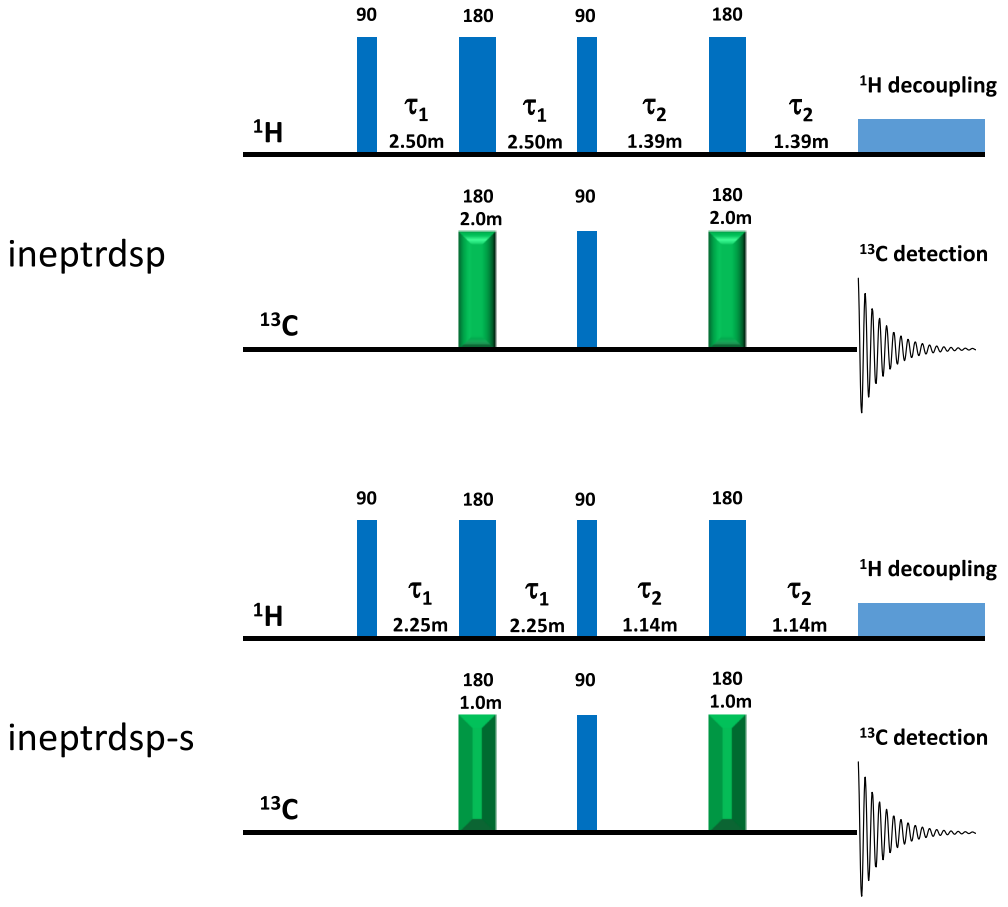

Figure 2. Pulse sequence of RINEPTSP (ineptrdsp) and RINEPTSP-S (ineptrdsp-s). τ_2 was optimized for CH_2.

enhancement is in high demand for studying increasingly complex polyolefin microstructures. We therefore offer several approaches to further enhance the sensitivity of a 10 mm high-temperature multinuclear cryoprobe. First, we report the extensive exploration of distortionless enhancement by polarization transfer (DEPT) and refocused insensitive nuclei enhanced by polarization transfer (RINEPT) for further boosting ^{13}C sensitivity. The use of hard, regular, and new short adiabatic 180° ^{13}C pulses in DEPT and RINEPT is investigated, including an example of analyzing saturated chain ends in an ethylene−octene (EO) copolymer sample with a hard 180° ^{13}C RINEPT pulse. Using $^{1}H-^{15}N$ HMBC to analyze the structure of a naturally abundant nitrogen-containing polyolefin is shown, which is difficult to achieve with a conventional probe. Finally, two technical challenges common to high-sensitivity NMR cryoprobes are also addressed: (1) good ^{1}H decoupling of ^{13}C NMR of polyolefin is essential, we show a new ^{1}H decoupling sequence Bi_Waltz_65_256pl to drastically reduce decoupling artifacts compared to "canned" decoupling sequences. (2) Acoustic ringing can cause problems affecting NMR spectral baseline (which can also affect sensitivity), especially on high-sensitivity cryoprobes. A simple solution is presented, while simultaneously producing quantitative results.

https://dx.doi.org/10.1021/acs.analchem.0c03753
Anal. Chem. 2020, 92, 15596−15603

EXPERIMENTAL SECTION

NMR standard reference samples were obtained from Bruker. Deuterium-labeled tetrachloroethane (TCE-d_2), tetrachloroethane, DMSO-d_6, and Cr(acac)$_3$ (Cr^{3+}) were obtained from Sigma-Aldrich and used without further purification. Polycat 15 was obtained from Evonik. Polyolefins were produced by Dow. Polyolefin terminated with methyl acrylate and capped with (2,2,6,6-tetramethylpiperidin-1-yl)oxyl (TEMPO) was provided by the University of Houston. NMR experiments were conducted on a Bruker AVANCE NEO or a Bruker AVANCE III HD 600 MHz system equipped with a multinuclear (C−Si−N−P/H) 10 mm high-temperature NMR cryoprobe. The sensitivities of different nuclei on this cryoprobe are listed and compared with those of several other cryoprobes in Table S1 in the Supporting Information. For experiments conducted at 120 °C, 10 min temperature equilibration time was used before tuning, matching, and data acquisition. Unless noted otherwise, raw NMR data were processed with Mestrelab Mnova software. Detailed NMR experimental parameters are listed in figure captions.

RESULTS AND DISCUSSION

Polarization Transfer to Increase ^{13}C Sensitivity. It is well-known that polarization transfer techniques, such as DEPT[22−24] and RINEPT,[25−27] can be used to increase the sensitivity of X-nuclei. The DEPT pulse sequence with hard 180° ^{13}C pulse (DEPTHP, Bruker pulse name "dept") and RINEPT with hard 180° ^{13}C pulse (RINEPTHP, Bruker pulse name "ineptrd") are shown in Figure S1. The sensitivity enhancement factors differ for CH, CH_2, and CH_3 groups at any θ degree pulse in "dept" and at any delay $T = 2 \times \tau_2$ in "ineptrd". To simplify the discussion, we will focus on sensitivity enhancement for CH_2 groups. Figure 1 shows the theoretical signal enhancement factors of "dept" and "ineptrd" for CH_2 with respect to θ or T. Clearly, sensitivities reach the maximum when θ in "dept" is 45° and T in "ineptrd" is 2 ms.

The sensitivity enhancements of DEPTHP, DEPT with an adiabatic 180° ^{13}C pulse (DEPTSP), RINEPTHP, and RINEPT with an adiabatic 180° ^{13}C pulse (RINEPTSP) for CH_2 groups were tested with a 5 mm C/H 600 MHz cryoprobe.[17] It was determined from a single measurement that the sensitivity enhancement sequence is RINEPTHP > RINEPTSP > DEPTHP > DEPTSP, and it was therefore recommended to use the RINEPTHP sequence for sensitivity enhancement of CH_2 groups in polyolefins.[17]

As compared with a 5 mm probe, B_1 radio frequency (rf) homogeneity is likely reduced in a 10 mm probe. Because an adiabatic 180° ^{13}C pulse is expected to excite uniformly across a larger ^{13}C chemical shift range than a 180° hard pulse,[28] we have systematically evaluated sensitivity enhancements of different DEPT (45°) and RINEPT sequences along with the application of different types of 180° ^{13}C refocusing pulses on the 10 mm multinuclear cryoprobe. The DEPT pulse sequences studied include DEPTHP, DEPTSP, and DEPTSP-S. DEPTSP-S is a short version of DEPTSP with 1 ms adiabatic 180° ^{13}C pulse (instead of 2 ms adiabatic 180° ^{13}C pulse) and with shape Crp80comp,1,20.4 (instead of Crp80comp4). RINEPT sequences studied include RINEPTHP, RINEPTSP, and RINEPTSP-S. RINEPTSP-S is a short version of RINEPTSP using the same adiabatic 180° pulse length and shape as DEPTSP-S described above, RINEPTSP and RINEPTSP-S pulses are shown in Figure 2.

An EO copolymer sample was run six times with each NMR pulse sequence, and then, the data were processed with Mnova software. Signal-to-noise ratios (S/Ns) were measured for peaks at (A) 40.22 ($\alpha\alpha$ peak), (B) 30.00 (EEE triad), and (C) 22.93 ppm ($2B_6$),[29] covering nearly the full CH_2 chemical shift range for common linear low density polyethylene (LLDPE). The average enhancement factors [enhancement factor = (S/N from polarization transfer pulse sequence)/(S/N from inverse gated zgig pulse sequence)] of the three peaks are shown in Figure 3. DEPTHP showed the highest enhancement factor among DEPT pulse sequences, primarily because of it being the shortest pulse sequence. It is well-known that long polarization transfer delays can result in relaxation losses and evolution of homonuclear couplings, and both result in impaired enhancements.[30] DEPTSP-S performed better than DEPTSP, again likely because of the shorter pulse sequence. We consistently observed that the DEPT pulse sequences produced minor phase distortions (Figure S2), which could come from the evolution of homonuclear couplings during long polarization delays. In direct comparison, RINEPT outperformed DEPT in every case we evaluated and could increase S/N by a factor of 3.1.

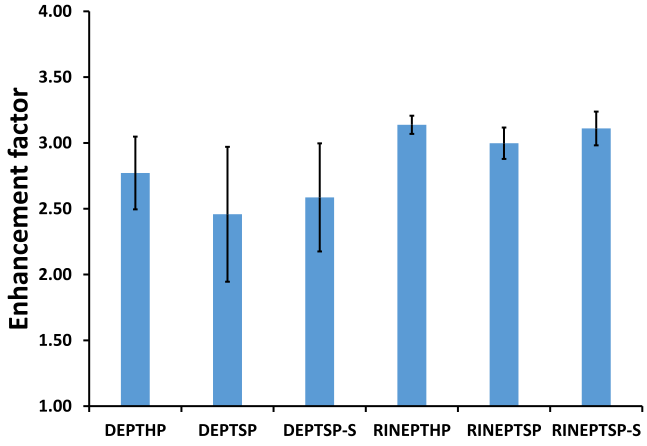

Figure 3. Enhancement factor of select CH_2 peaks with standard deviations from different NMR pulses. The sample is an EO copolymer in TCE-d_2 with 0.025 M Cr^{3+}. ^{13}C transmitter was set at 30.00 ppm. NS 1024. Noise range of 50−60 ppm was chosen.

To further evaluate the performances of different RINEPT pulses, S/N ratios of RINEPT sequences were analyzed with statistics software JMP "means/Anova" and "compare means with Student's t-test" analyses (Figure 4). The p-values we obtained here were 0.4651, 0.1498, and 0.2660 for peak A, B, and C, respectively. These p-values are all bigger than a significant level 0.05 that we set, and this can be taken as evidence that we cannot reject the null hypothesis that the means are the same. The cycles at right are from "compare means with Student's t-test", the cycles corresponding to RINEPTHP and RINEPTSP-S pulses turned red after clicking the cycle corresponding to RINEPTSP pulse. This means that although it seems RINEPTSP has lowest sensitivity enhancement in Figure 3, it is statistically not different from RINEPTHP and RINEPTSP-S for our sample studied here as shown in Figure 4. It is noted that the variation of S/N from RINEPTSP is the largest (Figure 4), plus it encodes the longest RINEPT pulse sequence which can be detrimental for systems with short relaxation times. We would recommend

https://dx.doi.org/10.1021/acs.analchem.0c03753
Anal. Chem. 2020, 92, 15596−15603

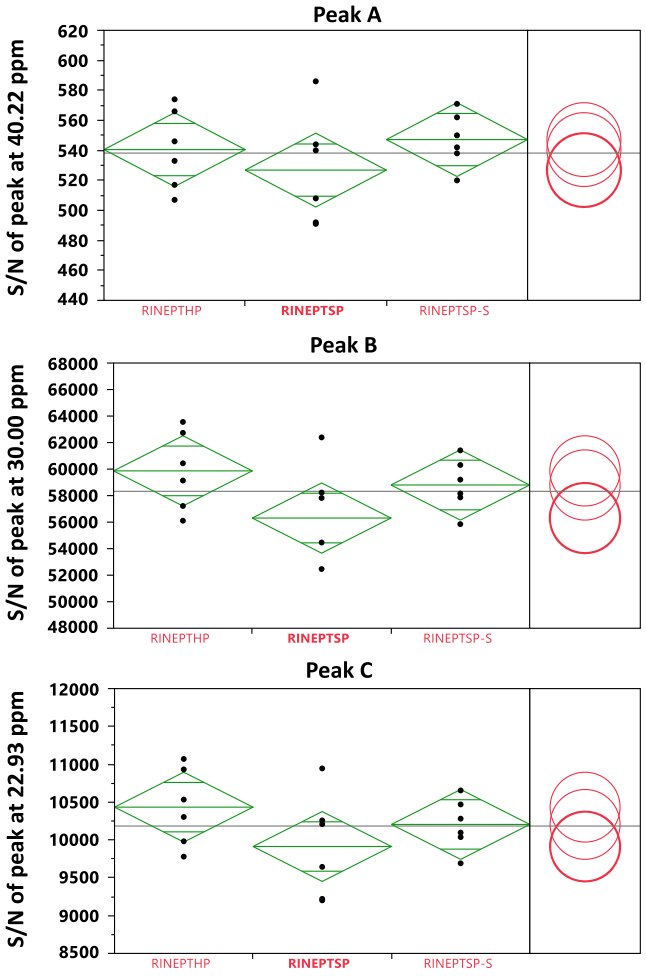

Figure 4. Statistic software JMP "means/Anova" and "compare means with Student's *t*-test" analyses of some CH_2 peaks' S/N obtained from different RINEPT pulse sequences. The sample is an EO copolymer in TCE-d_2 with 0.025 M Cr^{3+}. ^{13}C transmitter was set at 30.00 ppm. NS 1024. Noise range 50−60 ppm was chosen. Sample temperature is 120 °C.

using RINEPTSP-S when carbon atoms of interest have a larger chemical shift range. For normal LLDPE aliphatic carbon studies, such as measuring LCB, RINEPTHP is preferred.

The following example focuses on measuring a saturated chain end in an EO sample with RINEPTHP, which is preferred over RINEPTSP-S because this analysis involves a narrow ^{13}C chemical shift range. Analyzing saturated chain ends is very important for evaluating the polyolefin manufacturing process and catalyst performance. Despite being one of the most important LLDPEs, it is impossible to measure saturated chain ends in EO with ^{1}H NMR as the signals from EO side chain overlap with signals from the chain end. Halogenated naphthalenes were identified as good solvents to separate ^{13}C NMR signals of EO side chain from saturated chain end.[16] However, sensitivity is an issue as the concentration of polyolefin saturated chain ends is generally very low. It is necessary to further enhance the ^{13}C sensitivity beyond the 5.5× factor afforded by the cryoprobe itself [compared with a conventional broadband observe (BBO) probe] in order to measure the polyolefin saturated chain ends.[10] Figure 5 compares quantitative ^{13}C NMR on a 10 mm multinuclear NMR cryoprobe with the RINEPTHP pulse (a) and conventional NMR pulse on the same probe (b). The RINEPTHP experiment pulse delay is reduced by half compared with the conventional NMR pulse experiment because of faster proton relaxation.[17] Clearly, the ^{13}C NMR S/N with the conventional zgig pulse is well below the S/N = 10 denoting the limit of quantitation (LOQ) with a 53 min data acquisition time, whereas the corresponding S/N of the RINEPTHP pulse is well above LOQ with the same amount of acquisition time. To obtain similar S/N shown in Figure 5a one would need about 580 times longer acquisition time if using a conventional method and a 10 mm BBO probe ($5.5^2 \times 3.1^2 \times 2 \approx 580$. The factor 5.5 is from using cryoprobe, the factor 3.1 is from using RINEPT pulse, the last factor 2 is from reducing pulse delay when using RINEPT because of faster ^{1}H relaxation). The concentration of saturated chain end measured from Figure 5a is 0.20 chain ends per 1000 carbons with the calculation method described before and this method was validated with the result from conventional quantitative ^{13}C NMR zgig pulse sequence.[17]

NMR of Naturally Abundant Nitrogen-Containing Polyolefin. A polyolefin terminated with methyl acrylate and capped with TEMPO is shown in Figure 6. The goal was to determine if the TEMPO reagent is attached to the polymer chain as designed. Conventional NMR techniques, such as $^{1}H-^{1}H$ COSY, $^{1}H-^{13}C$ HSQC, $^{1}H-^{13}C$ HMBC and even diffusion NMR would have challenges to prove the TEMPO group attachment due to coresonance of both ^{1}H and ^{13}C signals from the TEMPO group and polyolefin chain. To achieve this goal, we explored $^{1}H-^{15}N$ HMBC (Figure 6). With an acquisition time of 1 h 28 min, three bond correlation peaks between protons "**a**" and "**b**" with nitrogen were clearly observed, although the concentration of TEMPO is very low and the TEMPO was not isotopically labeled. This result proved that the TEMPO group is connected to the polymer chain. To our knowledge, this is the first $^{1}H-^{15}N$ HMBC presented in the field of polyolefin characterization. The relative amount of the two similar structures is quantified to be 1.0:1.8 (**b**/**a**) by two-dimensional integration of $^{1}H-^{15}N$ HMBC, this ratio is supported with ^{1}H NMR data as the ^{1}H NMR peaks of **b** and **a** are almost separated. This $^{1}H-^{15}N$ HMBC approach provides a new way to quantify similar structures in case of proton peaks overlap, but ^{15}N chemical shifts are different.

Proton Decoupling on a High-Sensitivity NMR Cryoprobe. It is well-known that ^{1}H decoupling in ^{13}C NMR analysis of some polyolefins is very challenging with conventional decoupling sequences, such as Waltz-16.[31] Decoupling sidebands (cycling sidebands) are often present around the strong ^{13}C NMR signal of the methylene backbone, resulting in spurious peaks and inaccurate integrated intensities. These sidebands result from the periodic modulation of ^{13}C magnetization encoded in multipulse proton decoupling methods. These sidebands are a source of errors in composition and triad sequence distribution analyses by distorting the real intensities of related peaks. To reduce these sidebands, Zhou et al. have previously reviewed the efficacy of a 64-step bilevel implementation of Waltz-65 (Bi_Waltz_65_64pl).[32] However, 64-step is short of a full cycle of Waltz-65 and, accordingly, a 256-step bilevel implementation of Waltz-65 should be used. Decoupling artifacts are expected to increase in severity on high-sensitivity cryoprobes because ^{13}C S/N is significantly higher than it on a BBO probe.[32] We have, therefore, established a new

https://dx.doi.org/10.1021/acs.analchem.0c03753
Anal. Chem. 2020, 92, 15596−15603

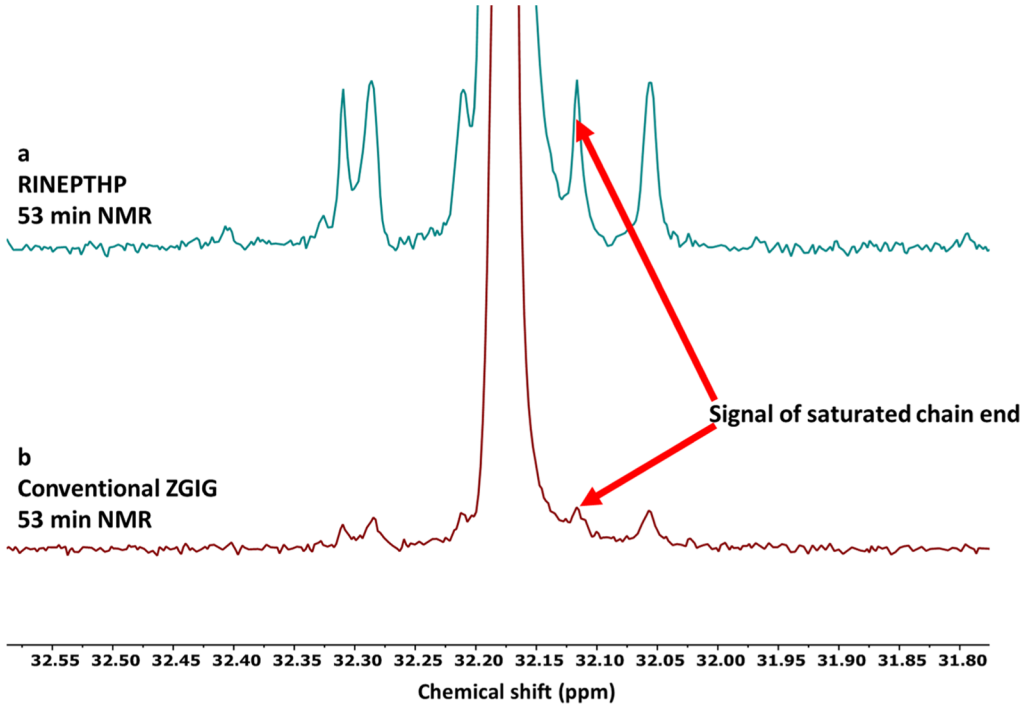

Figure 5. ^{13}C NMR of an EO sample in Cl-NA/PDCB-d_4 (9:1, w/w) containing 0.025 M Cr^{3+} with RINEPTHP pulse (a) and conventional zgig pulse (b). Sample temperature is 120 °C. ^{13}C transmitter was set at 32.00 ppm. Signal of saturated chain end was assigned based on ref 16.

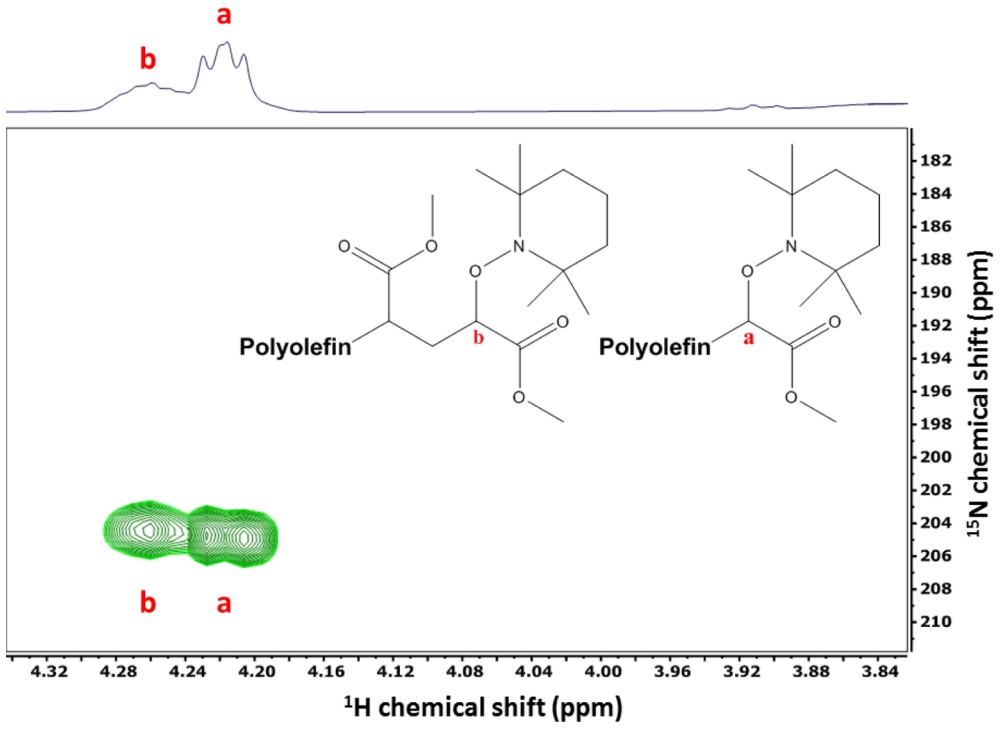

Figure 6. $^{1}H-^{15}N$ HMBC of a polymer with a 6-member ring functional group (part of the structure is shown). A total of 400 mg of the sample in 2.7 g of TCE-d_2, pulse sequence hmbcgplpndprqf, relaxation delay 1 s, number of scan 16, long-range $^{1}H-^{15}N$ coupling constant 6 Hz. Acquisition time 1 h 28 min.

Bi_Waltz_65_256pl decoupling sequence (Figure S3). The results of ^{13}C NMR spectra obtained with conventional Waltz-16 and the new Bi_Waltz-65_256pl decoupling sequences of a high-density polyethylene (HDPE) are compared in Figure S4. The spectrum using Bi_Waltz-65_256pl decoupling demonstrated no detectable artifacts in the range of interest from 7.0 to 48.0 ppm. Bi_Waltz-65_256pl sequence code in Bruker format and comparison of results with several different decoupling sequences along with Bi_Waltz-65_256pl are included in the Supporting Information (page S8 and Figure S5). It is worth noting that this Bi_Waltz-65_256pl decoupling sequence is suitable for a narrow window of ^{1}H decoupling

https://dx.doi.org/10.1021/acs.analchem.0c03753
Anal. Chem. 2020, 92, 15596−15603

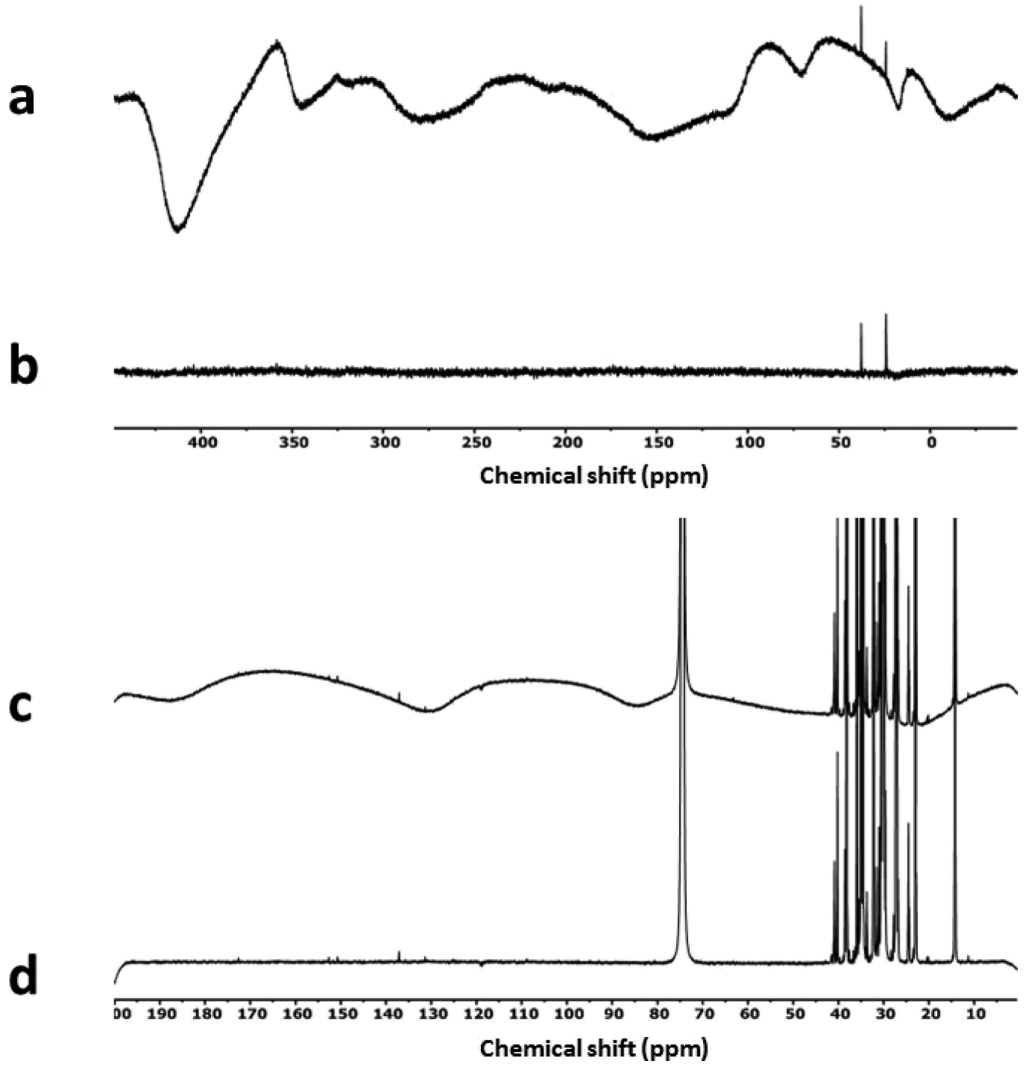

Figure 7. ^{15}N NMR spectra at 25 °C are shown in (a,b), 0.93 g Polycat 15 in 2.1 g DMSO-d_6, D_1 20 s, NS 2; ^{13}C NMR spectra at 120 °C are shown in (c,d), 200 mg of EO in 2.7 g of TCE-d_2 with 0.025 M Cr^{3+}, D_1 6 s, NS 1024. An inverse gated (zgig) pulse sequence was used for (a,c); a new inverse gated (zgig_pisp) pulse sequence shown in Figure 8 was used for (b,d).

such as that used in polyolefins. To decouple a wide chemical shift range of ^{1}H, a more general sequence such as Waltz-65 is a better choice.[32]

Baseline Issues on a High-Sensitivity Cryoprobe (Acoustic Ringing). It is well known that oscillating rf current in the circuit induces mechanical oscillations in metal parts of the cryoprobe when an NMR rf pulse is applied. These oscillations in turn generate rf signals in the receiver coil, which is often referred to as acoustic ringing. This acoustic ringing usually lasts tens to hundreds of microseconds after the NMR hard pulse, resulting in baseline distortion. This problem cannot be avoided by simply increasing the time between the last hard pulse and data acquisition (dead time) on high-sensitivity cryoprobes, especially for low frequency nuclei and wide spectral width. Figure 7 shows ^{15}N and ^{13}C NMR spectra of two samples with conventional inverse gated (zgig) pulse sequence (a,c), and ^{15}N and ^{13}C NMR spectra of the same samples with a new inverse-gated (zgig_pisp) pulse sequence (b,d). The zgig_pisp pulse sequence is shown in Figure 8 (sequence code in Bruker format can be found in the Supporting Information, page S15). Elimination of acoustic ringing effects observed in Figure 7a,c through the application

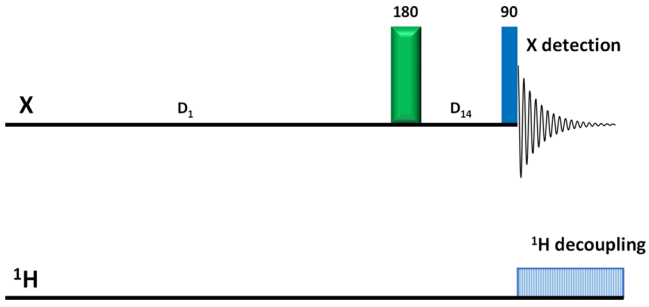

Figure 8. New inverse-gated pulse sequence zgig_pisp. The green bar represents an adiabatic 180° X pulses, which is only executed on even number of scans (i.e., only on scans 2, 4, 6, 8, ...). D_{14} 1.0 ms, Crp80,0.5,20.1 shape for adiabatic 180° is used.

of the zgig_pisp pulse sequence is clearly demonstrated in Figure 7b,d with dramatically flattened baselines. The approach applied here is to execute a 180° adiabatic shape pulse before the 90° hard X nucleus pulse on even number of scans, that is, scans, {2, 4, 6, 8, ...} = {2ℤ}, and acquire FID on opposite phase for odd and even number scans. The purpose of the 180° adiabatic shape pulse is to invert the NMR

https://dx.doi.org/10.1021/acs.analchem.0c03753
Anal. Chem. 2020, 92, 15596−15603

equilibrium magnetization to $-Z$ axis. By doing this, the baseline distortions are eliminated and signals from samples are accumulated as shown in Figure 7b,d.

The preservation of quantitative signal response with the new zgig_pisp sequences is important to point out. To demonstrate this, ^{13}C NMR data were collected at 120 °C for the EO sample (200 mg of EO in 2.7 g of TCE-d_2 with 0.025 M Cr^{3+}) with an inverse-gated pulse sequence (zgig) and the new inverse-gated pulse sequence (zgig_pisp). The ^{13}C NMR spectra were assigned based on Liu et al.[33] and the octene comonomer content was determined by solving the vector equation $\boldsymbol{s} = \boldsymbol{f} \times \mathbf{M}$ where $\mathbf{M}$ is an assignment matrix, $\boldsymbol{s}$ is a row vector representation of the spectrum, and $\boldsymbol{f}$ is a mole fraction composition vector as outlined by Qiu et al.[34] Then, the octene mol % contents from zgig pulse sequence and octene contents from zgig_pisp pulse sequence were analyzed with statistics software JMP modules "means/Anova" and "compare means with Student's *t*-test" (Figure S6), respectively. The statistical analysis concluded that the octene content determined using the conventional quantitative zgig and new zgig_pisp pulse sequences are the same. In other words, the zgig_pisp pulse sequence can be used to obtain flat baseline and quantitative results if correct pulse delays and other precautions are followed.[32]

CONCLUSIONS

DEPT and RINEPT pulse sequences with hard, regular, and new short adiabatic 180° ^{13}C pulses were explored on the 10 mm multinuclear cryoprobe for further increasing the ^{13}C sensitivity of polyolefin samples for minor structural characterizations. We recommend the new RINEPTSP-S sequence when carbon atoms of interest are distributed over a larger chemical shift range and RINEPTHP for normal LLDPE aliphatic carbon studies. Although the focus of the polarization transfer study here is CH_2 groups, the approach should also be applicable for CH and CH_3 groups in most polyolefins. The combination of a cryoprobe and RINEPT with optimized pulse delay can reduce acquisition time by a factor of 580 times when compared to conventional methods on a BBO probe. $^{1}H-^{15}N$ HMBC of natural isotope abundance polymers was demonstrated on a TEMPO-containing polyolefin using the multinuclear 10 mm cryoprobe. This approach is expected to be effective to analyze similar microstructures of other polymers. When using high-sensitivity cryoprobes, conventional ^{1}H decoupling sequences for ^{13}C NMR generate decoupling artifacts which result in inaccurate quantification of polyolefin microstructures. A new decoupling sequence, Bi_Waltz_65_256pl, was evaluated and shown to eliminate such artifacts. This decoupling sequence is suitable for a narrow chemical shift range ^{1}H decoupling such as aliphatic protons in polyolefins. To decouple a wider chemical shift range of protons, Waltz-65 is recommended. Finally, acoustic ringing is a general issue for high-sensitivity cryoprobes, which affects the NMR spectral baseline and sensitivity. To eliminate the problem while preserving quantitative properties, a new pulse sequence was reported.

ASSOCIATED CONTENT

Supporting Information

The Supporting Information is available free of charge at https://pubs.acs.org/doi/10.1021/acs.analchem.0c03753.

Sensitivities of different 600 MHz Bruker NMR cryoprobes; DEPT hard 180° ^{13}C pulse and RINEPT hard 180° ^{13}C pulse; ^{13}C NMR spectra obtained with different NMR pulse sequences; Bi_Waltz_65_256pl decoupling; ^{13}C NMR spectra of 200 mg of HDPE in 2.8 g of TCE-d_2 with 0.025 M Cr^{3+}; decoupling sequence Bi_Waltz-65_256pl (Bruker format); ^{13}C NMR spectra of a PE wax sample; decoupling effects of some decoupling sequences; pulse sequence zgig_pisp (Bruker format); and statistic software JMP "means/Anova" and "compare means with Student's *t*-test" analyses (PDF)

AUTHOR INFORMATION

Corresponding Authors

Zhe Zhou − *Dow, Lake Jackson, Texas 77566, United States;* orcid.org/0000-0003-0869-2112; Phone: 1-979-238-1387; Email: zzhou@dow.com; Fax: 1-979-238-0752

Rainer Kuemmerle − *Bruker Switzerland AG, CH-8117 Fällanden, Switzerland*; Phone: 41-44-825-9535; Email: rainer.kuemmerle@bruker.com; Fax: 41-44-825-9696

Authors

Nathan Rau − *Dow, Lake Jackson, Texas 77566, United States*

Donald Eldred − *Dow, Lake Jackson, Texas 77566, United States*

Aitor Moreno − *Bruker Switzerland AG, CH-8117 Fällanden, Switzerland*

Barbara Czarniecki − *Bruker Switzerland AG, CH-8117 Fällanden, Switzerland*

Xiaohua Qiu − *Dow, Lake Jackson, Texas 77566, United States*

Rongjuan Cong − *Dow, Lake Jackson, Texas 77566, United States*

Anthony P. Gies − *Dow, Lake Jackson, Texas 77566, United States;* orcid.org/0000-0002-3558-593X

Leslie Fan − *Dow, Lake Jackson, Texas 77566, United States*

Evelyn Auyeung − *Dow, Lake Jackson, Texas 77566, United States*

Dain B. Beezer − *Department of Chemistry, University of Houston, Houston, Texas 77204, United States*

Huong Dau − *Department of Chemistry, University of Houston, Houston, Texas 77204, United States*

Eva Harth − *Department of Chemistry, University of Houston, Houston, Texas 77204, United States*

Complete contact information is available at: https://pubs.acs.org/10.1021/acs.analchem.0c03753

Notes

The authors declare no competing financial interest.

ACKNOWLEDGMENTS

We would like to thank Profs. Jonathan V. Sweedler and Daniel Raftery for excellent suggestions regards contents. We would also like to thank Dr. Chen Peng for helpful discussions regarding Mnova data processing, and Drs. W. Konze, H. Boone, C. Li, R. Patel, B. Winniford, P. Chauvel, D. Meunier, E. Carnahan, M. Cheatham, L. Le, J. Klosin, Herb Praay, and Lake Jackson NMR team members at Dow for their support to this project.

REFERENCES

(1) Eagan, J. M.; Xu, J.; Di Girolamo, R.; Thurber, C. M.; Macosko, C. W.; Lapointe, A. M.; Bates, F. S.; Coates, G. W. *Science* **2017**, *355*, 814−816.
(2) Arriola, D. J.; Carnahan, E. M.; Hustad, P. D.; Kuhlman, R. L.; Wenzell, T. T. *Science* **2006**, *312*, 714−719.
(3) Hustad, P. D. *Science* **2009**, *325*, 704−707.
(4) Boelter, S. D.; Davies, D. R.; Milbrandt, K. A.; Wilson, D. R.; Wiltzius, M.; Rosen, M. S.; Klosin, J. *Organometallics* **2020**, *39*, 967−975.
(5) Boelter, S. D.; Davies, D. R.; Margl, P.; Milbrandt, K. A.; Mort, D.; Vanchura, B. A.; Wilson, D. R.; Wiltzius, M.; Rosen, M. S.; Klosin, J. *Organometallics* **2020**, *39*, 976−987.
(6) Hoult, D. I.; Richards, R. E. *J. Magn. Reson.* **1976**, *24*, 71−85.
(7) Kovacs, H.; Moskau, D.; Spraul, M. *Prog. Nucl. Magn. Reson. Spectrosc.* **2005**, *46*, 131−155.
(8) Banci, L.; Felli, I. C.; Kuemmerle, R. *Biochemistry* **2002**, *41*, 2913−2920.
(9) Ralph, J.; Lu, F. *Org. Biomol. Chem.* **2004**, *2*, 2714−2715.
(10) Zhou, Z.; Kümmerle, R.; Stevens, J. C.; Redwine, D.; He, Y.; Qiu, X.; Cong, R.; Klosin, J.; Montañez, N.; Roof, G. *J. Magn. Reson.* **2009**, *200*, 328−333.
(11) Zhou, Z.; Stevens, J. C.; Klosin, J.; Kümmerle, R.; Qiu, X.; Redwine, D.; Cong, R.; Taha, A.; Mason, J.; Winniford, B.; Chauvel, P.; Montañez, N. *Macromolecules* **2009**, *42*, 2291−2294.
(12) Frazier, K. A.; Froese, R. D.; He, Y.; Klosin, J.; Theriault, C. N.; Vosejpka, P. C.; Zhou, Z.; Abboud, K. A. *Organometallics* **2011**, *30*, 3318−3329.
(13) Cong, R.; deGroot, W.; Parrott, A.; Yau, W.; Hazlitt, L.; Brown, R.; Miller, M.; Zhou, Z. *Macromolecules* **2011**, *44*, 3062−3072.
(14) Zhou, Z.; Cong, R.; He, Y.; Paradkar, M.; Demirors, M.; Cheatham, M.; deGroot, A. W. *Macromol. Symp.* **2012**, *312*, 88−96.
(15) Zhou, Z.; Miller, M. D.; Lee, D.; Cong, R.; Klinker, C.; Huang, T.; Shan, C. L. P.; Winniford, B.; deGroot, A. W.; Fan, L.; Karjala, T.; Beshah, K. *Macromolecules* **2015**, *48*, 7727−7732.
(16) Zhou, Z.; Baugh, D.; Fontaine, P. P.; He, Y.; Shi, Z.; Mukhopadhyay, S.; Cong, R.; Winniford, B.; Miller, M. *Macromolecules* **2017**, *50*, 7959−7966.
(17) Zhou, Z.; Pesek, S.; Klosin, J.; Rosen, M. S.; Mukhopadhyay, S.; Cong, R.; Baugh, D.; Winniford, B.; Brown, H.; Xu, K. *Macromolecules* **2018**, *51*, 8443−8454.
(18) Zhou, Z.; Paradkar, R.; Cong, R.; Qiu, X.; Fan, L.; Kuemmerle, R.; Moreno, A.; Czarniecki, B. *Anal. Chem.* **2020**, *92*, 8350−8355.
(19) Osby, J.; Karjala, T.; Berbee, O.; Cooper, J. Ethylene-based polymers comprising unites derived from carbon monoxide and rheology modifying agent. U.S. Patent 10,654,955 B2, 2020.
(20) Hermel-Davidock, T.; Demirors, M.; Hayne, S.; Cong, R. Ethylene-based polymer compositions. U.S. Patent 8,729,200 B2, 2014.
(21) Effler, J.; Karjala, T.; Demirors, M.; Savargaonkar, R.; Bensason, S.; Zhou, Z. Process to produce enhanced melt strength ethylene/alpha-olefin copolymers and articles thereof. U.S. Patent 9,428,636 B2, 2016.
(22) Bendall, M. R.; Doddrell, D. M.; Pegg, D. T. *J. Am. Chem. Soc.* **1981**, *103*, 4603−4605.
(23) Doddrell, D. M.; Pegg, D. T.; Bendall, M. R. *J. Magn. Reson.* **1982**, *48*, 323−327.
(24) Schenker, K. V.; Von Philipsborn, W. *J. Magn. Reson.* **1986**, *66*, 219−229.
(25) Morris, G. A.; Freeman, R. *J. Am. Chem. Soc.* **1979**, *101*, 760−762.
(26) Burum, D. P.; Ernst, R. R. *J. Magn. Reson.* **1980**, *39*, 163−168.
(27) Sørensen, O. W.; Ernst, R. R. *J. Magn. Reson.* **1983**, *51*, 477−489.
(28) Hou, J.; He, Y.; Qiu, X. *Macromolecules* **2017**, *50*, 2407−2414.
(29) Qiu, X.; Redwine, D.; Gobbi, G.; Nuamthanom, A.; Rinaldi, P. L. *Macromolecules* **2007**, *40*, 6879−6884.
(30) Heikkinen, S.; Toikka, M. M.; Karhunen, P. T.; Kilpeläinen, I. A. *J. Am. Chem. Soc.* **2003**, *125*, 4362−4367.
(31) Seger, M. R.; Maciel, G. E. *Anal. Chem.* **2004**, *76*, 5734−5747.
(32) Zhou, Z.; Kümmerle, R.; Qiu, X.; Redwine, D.; Cong, R.; Taha, A.; Baugh, D.; Winniford, B. *J. Magn. Reson.* **2007**, *187*, 225−233.
(33) Liu, W.; Rinaldi, P. L.; McIntosh, L. H.; Quirk, R. P. *Macromolecules* **2001**, *34*, 4757−4767.
(34) Qiu, X.; Zhou, Z.; Gobbi, G.; Redwine, O. D. *Anal. Chem.* **2009**, *81*, 8585−8589.

https://dx.doi.org/10.1021/acs.analchem.0c03753
Anal. Chem. 2020, 92, 15596−15603